

## Steam oxidation of ferritic steels: kinetics and microstructure

A. ARÍZTEGUI, T. GÓMEZ-ACEBO, F. CASTRO

CEIT y Escuela Superior de Ingenieros Industriales  
Paseo Manuel de Lardizábal, 15 – 20018 San Sebastián (Spain)

The ferritic 2.25Cr–1Mo steel has been subjected to isothermal and non-isothermal oxidation treatments in water steam at several temperatures ranging from 550 to 700 °C for up to 56 days. Under isothermal conditions this steel follows a parabolic oxidation kinetics, with an activation energy of 324 kJ mol<sup>-1</sup>. This value corresponds to an apparent activation energy for the global process, which includes both outward diffusion of Fe cations and inward diffusion of oxygen.

The oxidation products present in the oxide scales, which were characterised by X-ray diffraction and SEM, are in total agreement with the Fe-O phase diagram. Thus, magnetite is the most stable oxide at low temperatures and wustite starts to form above 570 °C. Further studies of the effect of cooling rate have shown that wustite formed at 700 °C transforms into magnetite during a slow cooling, whereas a rapid cooling inhibits this transformation to a certain extent.

For non-isothermal oxidation treatments consisting of a holding period at 550 °C followed by a single or double 4 hours exposure at 700 °C, the oxidation process seems to occur in sequence, thus presenting an additive effect of the oxidation treatments carried out at each temperature. This effect was observed both, for the type of oxide grown, and for the kinetics of the process. Microscopic observations of the oxide scales formed after the various oxidation treatments revealed that the oxide scales are constituted by sublayers of distinct microstructure and chemical composition changing from their surface to the substrate interface.

*Keywords: Ferritic steel, isothermal and non-isothermal oxidation, kinetics, diffusion mechanism.*

### Oxidación de aceros ferríticos con vapor de agua: cinética y microestructura

Se han realizado tratamientos de oxidación isoterma y no isoterma a un acero ferrítico 2,25Cr–1Mo en vapor de agua, a temperaturas comprendidas entre 550 y 700 °C y tiempos de hasta 56 días. En condiciones isotermas, este acero tiene una cinética de oxidación parabólica, con una energía de activación de 324 kJ mol<sup>-1</sup>. Este valor corresponde a una energía de activación aparente del proceso global, que incluye tanto la difusión hacia el exterior de cationes de Fe, como la difusión de oxígeno hacia el interior. Los productos de oxidación presentes en la capa de óxido, caracterizados por difracción de rayos-X y SEM, están en total concordancia con el diagrama de fases del sistema Fe-O. La magnetita es el óxido más estable a bajas temperaturas, y la wustita comienza a formarse por encima de 570 °C. Estudiando el efecto de la velocidad de enfriamiento se ha comprobado que la wustita formada a 700 °C se transforma en magnetita en un enfriamiento lento, mientras que el enfriamiento rápido inhibe en parte esta transformación.

En los tratamientos de oxidación no isoterma, consistentes en un periodo de mantenimiento a 550 °C seguido de exposición simple o doble a 700 °C, el proceso de oxidación parece producirse secuencialmente, presentando así un efecto aditivo de los tratamientos de oxidación realizados a cada temperatura. Este efecto se ha observado tanto por el tipo de óxido formado como por la cinética del proceso. Las observaciones en el microscopio del óxido formado en los diversos tratamientos de oxidación, revelan que la capa de óxido está formada por subcapas de diferente microestructura y composición química, variando desde su superficie hasta la intercara con el sustrato.

*Palabras clave: acero ferrítico, oxidación isoterma y no isoterma, cinética, mecanismo de difusión.*

### 1. INTRODUCTION

Ferritic steels are commonly used for superheaters and reheaters of power generating plant boilers. Therefore, it is important to gain a clear understanding of the oxidation behaviour of these materials at high temperatures in contact with water steam.

Although extensive research has been conducted (1-14) to study the oxidation behaviour of steels under various atmospheres, these studies have been generally carried out under isothermal conditions. However, during operation of the power generating plant the tubes are not strictly subjected to a constant temperature during their life in service. This is the reason why during the present work the experimental T22 steel (containing 2.25% Cr – 1% Mo) has been studied considering both, isothermal and non-isothermal oxidation treatments.

As a baseline for comparison, the steel was initially subjec-

ted to isothermal oxidation treatments in contact with water steam for 7 to 56 days, within a temperature range between 550 and 650 °C. Additionally, a number of specimens were exposed to a temperature of 700 °C for up to 24 hours, comparing the effect of rapid and slow cooling. On the other hand, the non-isothermal experiments consisted of thermal cycles at 550 °C followed by exposure at 700 °C for a predetermined length of time. The fact that these temperatures were also used to study the oxidation kinetics of this steel under isothermal conditions allowed to analyse the effect of their combination during the non-isothermal treatments.

The characterisation of the oxidation kinetics was carried out through measurements of both, the oxide scale thickness and weight gains of the steel samples, as a function of time and temperature.

## 2. EXPERIMENTAL PROCEDURE

Oxidation tests were carried out using T22 steel tubes (19.05 mm outside diameter, 2.27 mm wall thickness, 140 cm long) whose chemical composition is 0.085 C, 0.54 Mn, 0.32 Si, 0.022 P, 0.013 S, 2.09 Cr, 0.14 Ni, 0.97 Mo, 0.26 Cu, 0.011 Al, 0.019 Sn, Fe-bal.

In order to obtain precise values of weight gain per unit surface area, small specimens were placed inside the tubes at fixed positions. These samples were cut from the T22 tubes into rectangular specimens measuring 2x1.3x2 mm in size. They were subsequently polished to 1 $\mu$ m finish on the upper surface and weighed before and after oxidation to an accuracy of 10<sup>-4</sup> g.

The layout of the experimental device used is shown in Fig. 1. A constant flux of high purity argon (99.999 % pure) used as a water steam carrier was established and fed through three conducts, each one provided with a flow-regulating valve. One stream reached directly the "reference tube" in the furnace in order to have a reference oxidation in the absence of water steam. The other two argon streams flowed through a water flask (containing high purity distilled water) before reaching the furnace. Water was set at a constant temperature (between 60 °C and 100 °C) by a rheostat to give the desired steam partial pressure. Good contact was assured between water and argon by passing the gas through a porous membrane situated at the bottom of the flask. The most appropriate temperature to obtain a regular oxidation along the length of the tube was determined to be ~ 90 °C (70.1 kPa).

Condensation in the pipework between the flasks and furnace was prevented by installing heating wires to a temperature above 100 °C. Once in the furnace, the three gas flows were circulated inside the tubes undergoing oxidation. Before assembly, the tubes were chemically cleaned to remove oxide and grease.

The outgoing gases were then guided, using a coil made of copper tubing, in order to reduce their temperature. The gases were subsequently passed through a liquid mixture of oil and silicone where they form bubbles, which consequently reach the environmental atmosphere. This arrangement totally avoids the entrance of oxygen through the final end of the tubes.

Before starting the oxidation treatment all air was flushed out from the system during 2 days, in order to eliminate any remaining oxygen in the system.

Temperature uniformity within the tubes was also verified and assured through the use of thermocouples. Test specimens were therefore placed aside the temperature measuring points.

Several samples were cut from each tube to be metallographically analysed after polishing. The thickness of the oxide scale formed at the inner surface of the experimental steel tubes and specimens was measured by SEM on carefully prepared cross sections.

The oxidized rectangular specimens were also weighed, in order to measure the weight gain per unit area as a function of time and temperature. XRD was performed directly on the surface of the specimens, to characterise the phases present in the oxide products. As this method gives information on compounds present in the top ~10 $\mu$ m of the oxide layer, after the first scan, some scales were carefully polished to be scanned again.

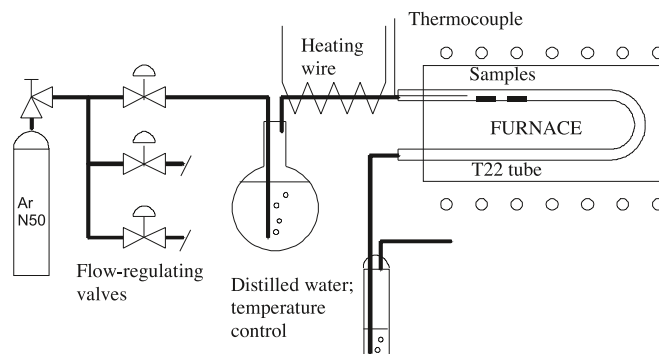


Figure 1: Schematic illustration of the steam oxidation testing device.

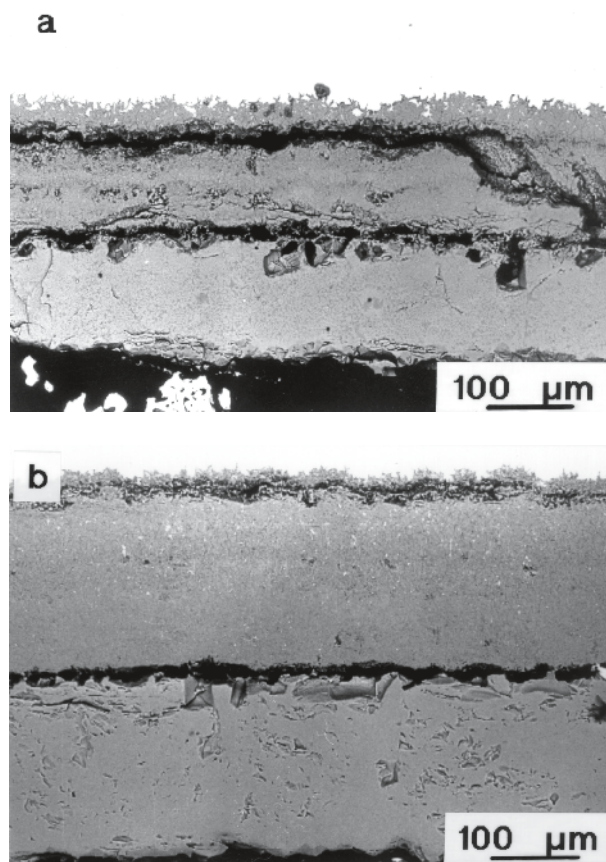


Figure 2: SEM micrographs of oxide scales after 28 days at (a) 625°C and (b) 650°C.

## 3. RESULTS AND DISCUSSION

### 3.1. Isothermal oxidation

The experimental tubes and specimens were subjected to isothermal oxidation for up to 56 days within the temperature range of 550 °C to 650 °C. In agreement with previous reports (1), after oxidation of the ferritic T22 steel, a double oxide layer was observed, regardless of time and temperature of the oxidation. Fig. 2 shows the appearance of the sections of the oxide scales as the oxidation temperature is increased.

As previously reported by other authors (2-5), the data collected for the thickness of the oxide scale after the oxida-

tion experiments carried out in this work and summarised in Fig. 3, showed that the 2.25%Cr – 1%Mo steel follows a parabolic oxidation kinetics within the experimental oxidation temperature range and an oxidation time of up to 56 days.

A linear regression of the experimental data points leads to a reasonable fit of straight lines through the origin, represented by the equation

$$d^2 = k_p t \quad [1]$$

where  $d$  is the total thickness of the oxide layer and  $t$  the oxidation time. The parabolic oxidation rate constant  $k_p$  ( $\text{m}^2 \text{s}^{-1}$ ) is given by

$$k_p = k_0 \exp(-Q / RT) \quad [2]$$

where  $Q$  is the activation energy of the process,  $R$  the gas constant, and  $T$  the absolute temperature. Using equation [2] and plotting the data as shown in Fig. 4 yields a value of an apparent activation energy for oxidation of  $Q = 324 \text{ kJ mol}^{-1}$ . Likewise, the activation energy of the process determined from the weight gain data gives a value of  $308 \text{ kJ mol}^{-1}$ . This activation energy corresponds to the global process. Since in general the activation energy of an oxidation process is related to the basic diffusion mechanisms taking place, this value is interpreted as an apparent oxidation activation energy considering both outward diffusion of Fe ions and inward diffusion of O ions. This value closely agrees with values reported by other authors (5, 6) and is consistent with a reaction controlled by diffusion during which passivation of the metal takes place thus leading to a parabolic oxidation kinetics.

The oxide scales were characterised by X-ray diffractometry. Results are summarised in Table I, which shows that magnetite is formed at any temperature between 550 and 650 °C, after exposures to hot water steam for up to 56 days. However, for oxidation temperatures higher than 570 °C (stabilisation temperature of FeO) wustite starts to form beneath the magnetite layer. This observation is also confirmed by the phase diagram in Fig. 5. At 650 °C the wustite layer is already detected in the first scan (that is, it is at the surface of the oxide scale) and the  $\text{Fe}_3\text{O}_4/\text{FeO}$  ratio seems to decrease which indicates that as the oxidation temperature is increased FeO becomes stable and the amount present in the oxide layer increases. Its formation may be interpreted associated to a reaction between oxygen and Fe at the reaction interface:

i) oxygen permeated through oxide layer ( $\text{Fe}_3\text{O}_4$ ) to react with Fe ( $\text{Fe} + \text{O} \rightarrow \text{FeO}$ ), or alternatively by an

ii) internal reaction between previous  $\text{Fe}_3\text{O}_4$  and Fe ( $\text{Fe}_3\text{O}_4 + \text{Fe} \rightarrow \text{FeO}$ ) due to destabilisation of the  $\text{Fe}_3\text{O}_4$  at high temperature.

Both arguments explain why FeO is nearly always found in contact with the Fe reaction interface, which also supports the fact that at low oxygen concentrations FeO is more stable than  $\text{Fe}_3\text{O}_4$  since it is an oxide that requires less oxygen to be formed.

Also at high temperatures ( $T_{\text{oxid}} > 570 \text{ °C}$ ) there seems to be an evolution in time of the oxide layers to stabilise FeO rather than  $\text{Fe}_3\text{O}_4$  even altering its relative position within the oxide layer, thus leading to a mixture of both phases in the oxide layer.

Besides, at extremely high temperatures (e.g.  $T_{\text{oxid}} \sim 700 \text{ °C}$ ) the only oxide species found is FeO with total absence of  $\text{Fe}_3\text{O}_4$ . Experiments were carried out for up to 24 hours. This again is in total agreement with the fields of stability shown

TABLE I: OXIDE PRODUCTS PRESENT IN THE OXIDE SCALES FORMED, AS IDENTIFIED BY XRD, AFTER ISOTHERMAL OXIDATION TREATMENTS UNDER VARIOUS COMBINATIONS OF TIME AND TEMPERATURE. M: MAGNETITE, H: HEMATITE, W: WUSTITE.

	550 °C	600 °C	625 °C	650 °C
7 days	M + H	M/W	M	W/M+W
14 days	M + H	M	M + (W)	/
28 days	M + H	M	M + W	M + W
56 days	M	M	M + W	/

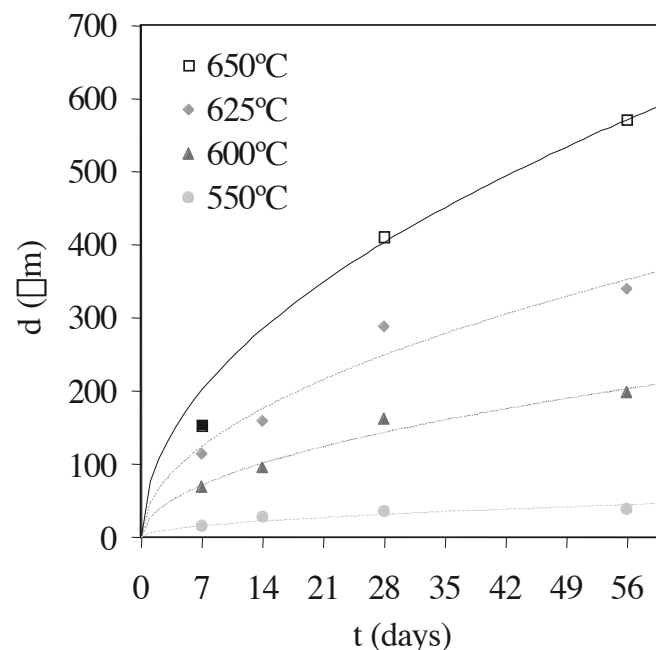


Figure 3: Scale thickness as a function of oxidation time at various temperatures.

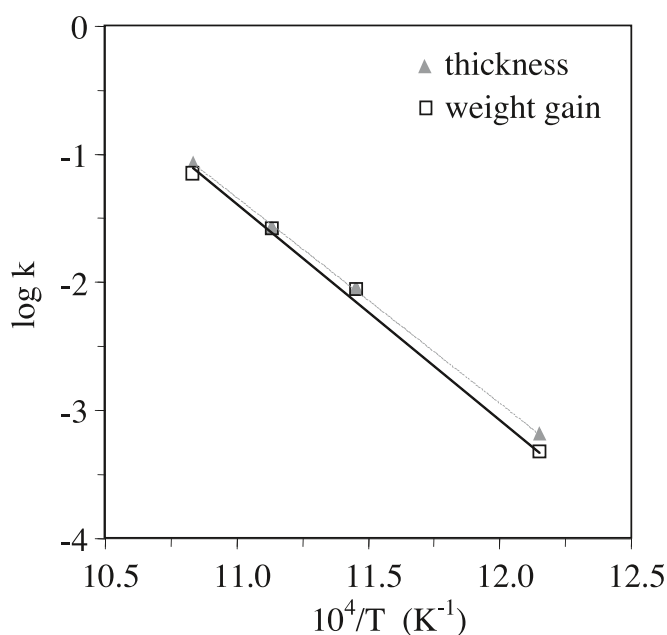


Figure 4: Arrhenius plot for the parabolic rate constant of oxidation as a function of absolute temperature.



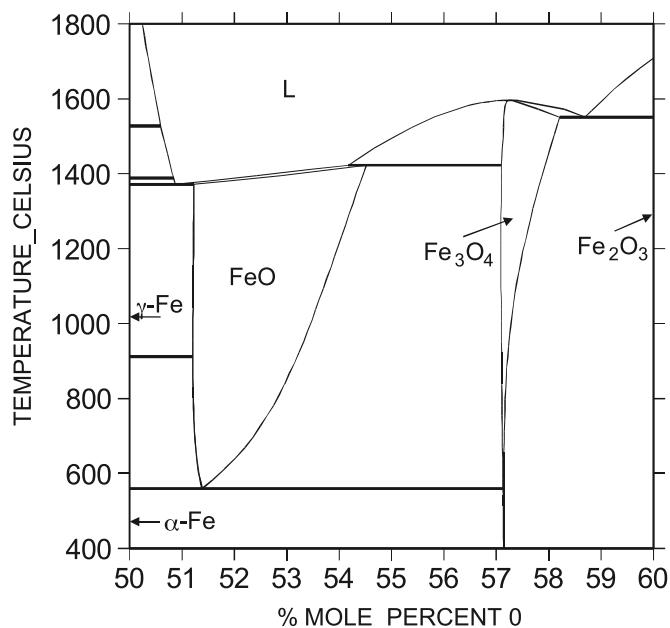


Figure 5: The iron - oxygen phase diagram.

by the phase diagram in Fig. 5.

Thus summarising it could be said that,

1) If  $T \gg 570\text{ }^{\circ}\text{C} \rightarrow \text{FeO}$  is directly formed from the beginning of the oxidation process.

2) If  $T > 570\text{ }^{\circ}\text{C} \rightarrow \text{FeO}$  tends to be formed but local oxidation conditions (cold spots or locally oxygen rich atmosphere) also gives rise to  $\text{Fe}_3\text{O}_4$ .

3) If  $T \leq 570\text{ }^{\circ}\text{C} \rightarrow \text{Fe}_3\text{O}_4$  is stable and no formation of  $\text{FeO}$  is observed.

4) Additionally oxidation time seems to have less influence than temperature i.e., although oxide formation is diffusion controlled, there seems to be a need for a high thermal activation of the process to lead to the formation of  $\text{FeO}$ .

A few oxidation experiments were performed in order to compare the effect of a rapid or slow cooling from  $700\text{ }^{\circ}\text{C}$ . Although thickness or weight gain data were not affected by the different ways of cooling, the type of oxide was directly related to it: when rapidly cooled, the only oxide found was wustite, whereas with slow cooling also magnetite was formed. This observation indicates that wustite may transform into magnetite during cooling. This process takes place by oxygen diffusion in order to adapt the  $\text{FeO}$  to the new structure of the  $\text{Fe}_3\text{O}_4$ . Atomic movement will therefore be needed to cause transformation of the oxide from a stoichiometric cell of 2 atoms per unit cell to one containing 7 atoms per cell. This is therefore a diffusion controlled transformation as suggested by previous reports (6, 7).

Scanning electron micrographs in Fig. 6 show the surface morphologies of the oxide scales formed at different temperatures. Fig. 6a was identified by XRD as magnetite and Fig. 6b as magnetite plus hematite (see table I). As magnetite presents a porous aspect, the fine needles observed in Fig. 6b are attributed to hematite. Finally, Fig. 6c corresponds to wustite.

It can also be seen that both layers grow to almost identical thickness, the inner layer consisting of fine, equiaxed grains, whereas the outer layer presents a columnar structure (Fig. 7). Many investigations of duplex growth using inert markers (8, 10, 12) show that the boundary between the layers corresponds to the position of the original metal surface, which may

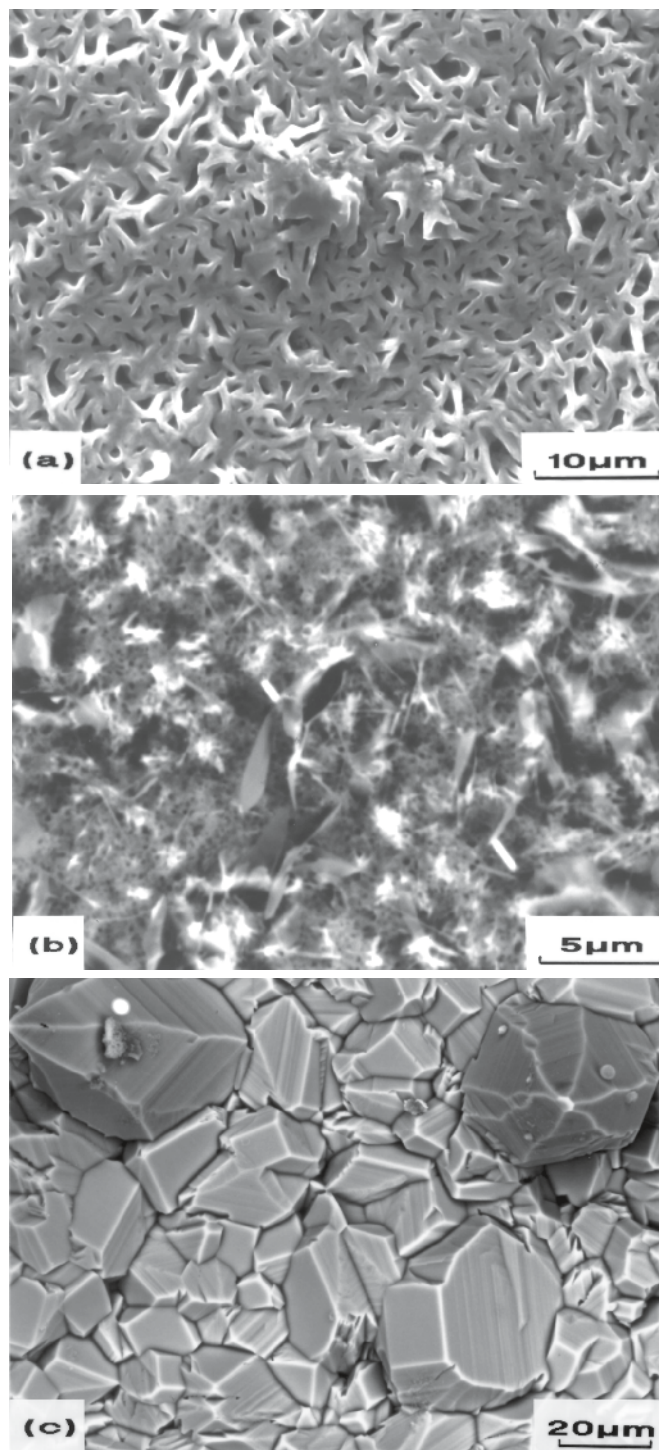


Figure 6: SEM micrographs showing the surface appearance of different oxide layers exhibiting (a) magnetite, (b) magnetite plus hematite, (c) wustite.

indicate that the inner layer grows from the original metal-oxide interface by inward oxygen diffusion, while the outer layer grows towards the oxide-gas interface by outward diffusion of iron cations. This is in agreement with EDS and mapping scans taken from cross-sections through the oxide layer, which revealed that the alloying elements present in the steel are only found in the inner layer. This is illustrated in Fig. 8, which corresponds to the concentration profile for Cr. This diagram not only shows that the concentration of Cr is extre-

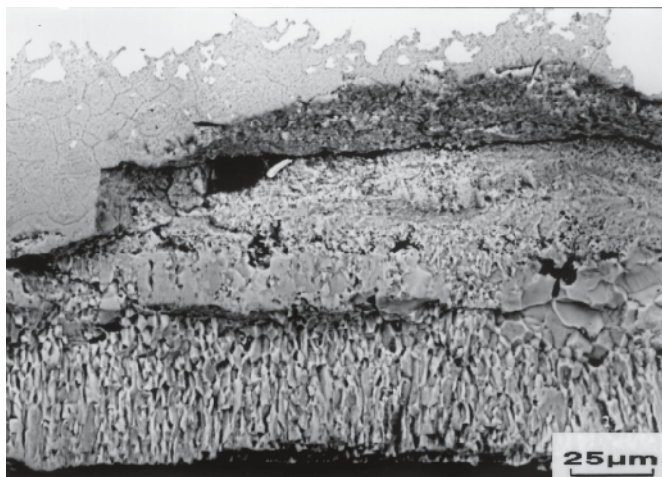


Figure 7: Fracture surface of the oxide scale formed after 7 days at 625°C.

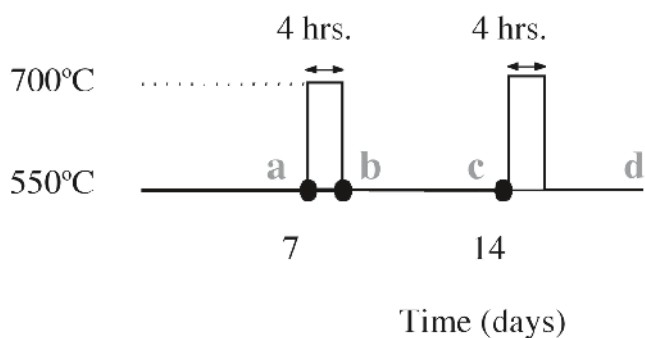


Figure 9: Scheme of the oxidation cycles under non-isothermal conditions.

mely low in the outer oxide layer, but also that the inner layer contains nearly twice as much Cr than the steel substrate itself. This observation confirms again the outward diffusion of Fe cations during the oxidation process thus leading to an apparent Cr enrichment in an area (inner oxide layer) previously occupied by the steel substrate.

**3.2. Non-isothermal oxidation**

As stated before, the operation conditions of a power plant does not always take place at constant temperatures, e.g. because of transients, overshootings or even the presence of hot spots. Simulation of non-isothermal oxidation conditions was therefore undertaken as part of this study.

The basic non-isothermal oxidation cycles consisted of a week at 550 °C followed by a period between 8 or 24 hours at 700 °C. The effect of both slow and rapid cooling was studied after the holding period at 700 °C. Another series consisted of a week at 550 °C followed by 4 hours at 700 °C and one more week at 550 °C. Also another cycle including a second holding period at 700 °C was used. These cycles are schematically illustrated in Fig. 9, and the results obtained were compared to those corresponding to the isothermal oxidation treatments.

After non-isothermal treatments the oxide scales formed were very irregular and evidently cracked due to differences in thermal expansion between the oxide layer and the sub-

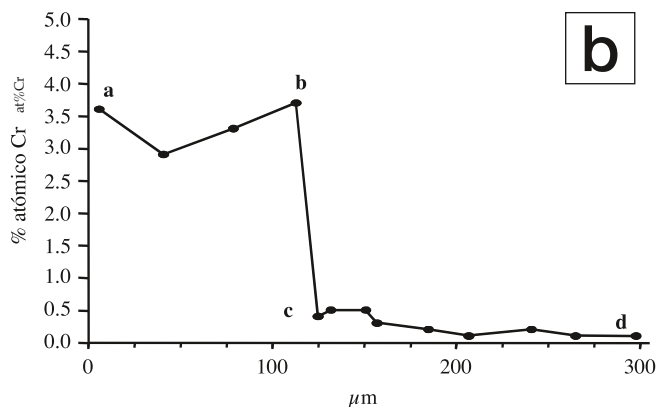
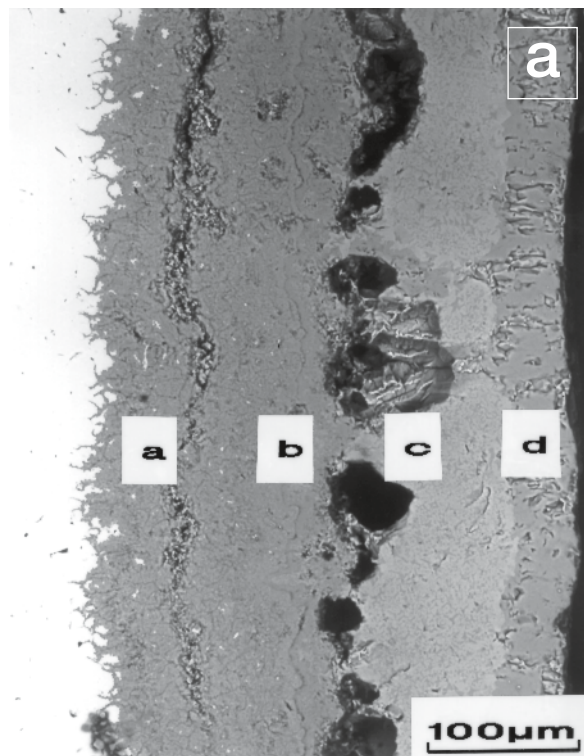


Figure 8: Concentration profile for Cr on a cross-section of the oxide scale formed after 56 days at 625°C.

trate. For this reason measurements of oxide thickness were complicated, thus, being more accurate to use weight gain as a record of the oxidation kinetics. Fig. 10 shows the results obtained after both, isothermal and non-isothermal treatments. As described by the oxidation cycle (Fig. 9), point **b** is obtained after 1 week at 550 °C plus 4 hours at 700 °C. The total weight gain is actually the sum of the results separately obtained after both oxidation treatments, thus exhibiting an additive effect. However, points **c** and **d** indicate an oxidation kinetics which closely follows that one of the isothermal treatment. In fact, this means that a second “peak” at 700 °C does not have an additional effect on the oxidation kinetics, which may therefore evidence the passivating character of the oxide scale formed during the previous non-isothermal treatment.

In terms of the phases contributing the oxide scales, the X-ray diffraction patterns (table II) reveal that below the layer of magnetite, grown during a week at 550 °C (table I), wustite



TABLE II: OXIDE PRODUCTS PRESENT IN THE OXIDE SCALES FORMED, AS IDENTIFIED BY XRD, AFTER NON-ISOTHERMAL OXIDATION TREATMENTS UNDER VARIOUS COMBINATIONS OF TIME AND TEMPERATURE.  
M: MAGNETITE, H: HEMAITITE, W: WUSTITE.

550 °C + 700 °C	Slow cooling	Rapid cooling
7 days + 4 h	M/M+(W)	M/M+(W)
7 days + 8 h	/	M/M+W
7 days + 24 h	M/M+W	M+W/W+M
7 days + 4 h + 7 days 550 °C	M+H/M	/

is formed during the oxidation time at 700 °C. Besides, the longer the time at 700 °C (4, 8, 24 hours), the larger the amount of wustite formed. From this observation it may therefore be concluded that the magnetite outer layer is permeable to oxygen diffusion, since wustite is formed as a result of the reaction between oxygen and iron on the original surface of the steel. The stability of wustite was also observed to be affected by the cooling rate since oxidation after 7 days at 550 °C plus 24 hours at 700 °C, followed by rapid cooling leads to an oxide scale constituted by a newly formed wustite at the reaction interface on the steel substrate located beneath the magnetite layer. In contrast, after slow cooling the wustite layer was observed to exhibit magnetite grains as a result of the time dependent transformation (see figures 11 and 12). Besides, after 7 days at 550 °C the whole of the wustite layer formed at high temperature was transformed to magnetite.

#### 4. CONCLUSIONS

The isothermal oxidation kinetics of the studied steel was observed to be of a parabolic type in all the experimental temperature range and up to 56 days. Therefore, in spite of the microstructural difference of the oxide layers formed on the surface of the steel at different temperatures, their net effect is to act passivating the steel.

The results obtained for the oxidation kinetics of the steel after a non-isothermal treatment are equivalent to the sum of the kinetics corresponding to a sequence of isothermal oxidation treatments carried out at those respective temperatures.

In general the microstructure of the oxide scales exhibits a gradient of the oxidation products so producing a layered structure essentially composed by wustite and magnetite. For non-isothermal treatments the relative amount of these constituents seems to be dependent on the cooling rate and the oxidation treatment temperature. The type of iron oxide formed at different temperatures is in total agreement with the iron-oxygen phase diagram

#### ACKNOWLEDGEMENTS

An acknowledgement is emphasised to IBERDROLA for the economic support for the realisation of this work.

#### REFERENCES

1. J. Robertson, "The mechanism of high temperature aqueous corrosion of steel", *Corrosion Sci.* **29**, 1275-1291 (1989).
2. P. L. Surman and J. E. Castle, "Gas phase transport in the oxidation of Fe and steel", *Corros. Sci.* **9**, 771-777 (1969).
3. I. E. Klein, J. Sharon and A. E. Yaniv, "A mechanism of oxidation of ferrous alloys by super-heated steam", *Scripta Metall.* **15**, 141-144 (1981).

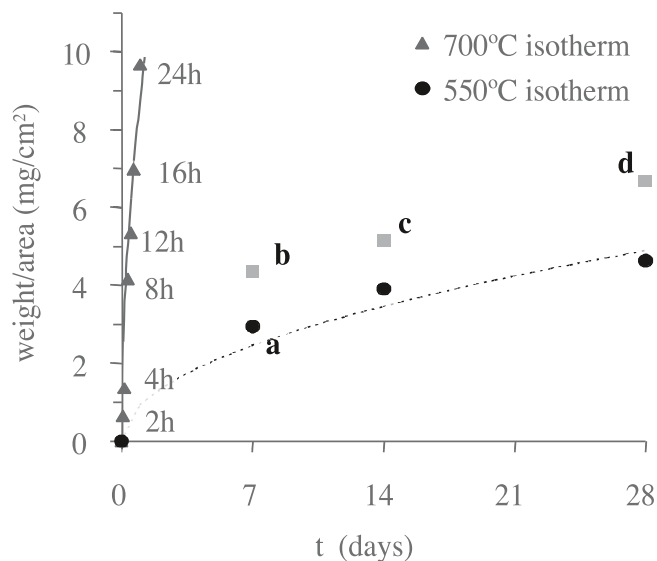


Figure 10: Oxidation kinetics after isothermal treatments, at 550 and 700°C. For comparison purposes, points b, c and d are included corresponding to non-isothermal treatments as represented in figure 9.

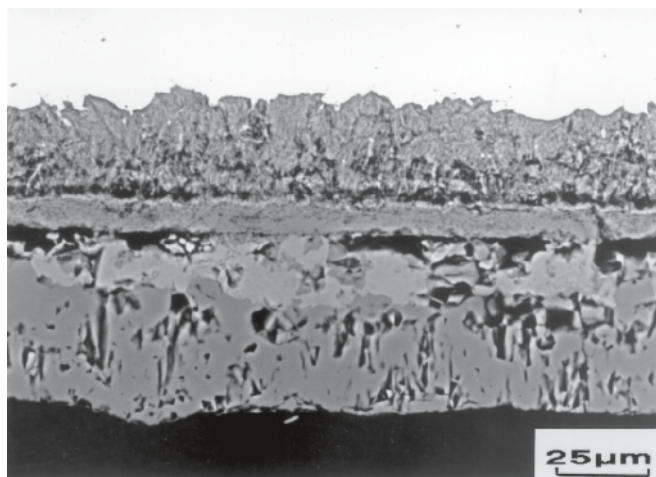


Figure 11: SEM micrograph of the oxide scale formed after 7 days at 550°C plus 24 hours at 700°C followed by slow cooling.

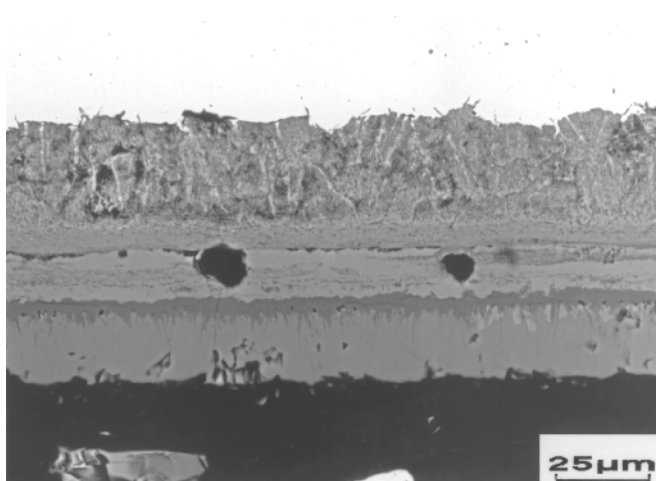


Figure 12: SEM micrograph of the oxide scale formed after 7 days at 550°C plus 24 hours at 700°C followed by rapid cooling.

4. L. Tomlinson and N. J. Cory, "Hydrogen emission during the steam oxidation of ferritic steels: kinetics and mechanism", *Corros. Sci.* **29**, 939-965 (1989).
5. T. Sumida, T. Ikuno, N. Otsuka, T. Saburi, "High temperature oxidation behaviour of 2.25% Cr - 1% Mo steel boiler tubes in long-term exposure to superheated steam", *Mater. Trans., JIM*, **36**, 1372-1378 (1995).
6. H. T. Abuluwefa, R. I. L. Guthrie and F. Ajersch, "Oxidation of low carbon steel in multicomponent gases: Part I. Reaction mechanisms during isothermal oxidation", *Metall. Mater. Trans. A*, **28A**, 1633-1641 (1997).
7. J. S. Sheasby, W. E. Boggs and E. T. Turkdogan, "Scale growth on steels at 1200°C: rationale of rate and morphology", *Met. Sci.* **18**, 127-136 (1984).
8. A. Brückman, "The mechanism of transport of matter through the scales during oxidation of metals and alloys", *Corros. Sci.* **7**, 51-59 (1967).
9. S. Mrowec, "On the mechanism of high temperature oxidation of metals and alloys", *Corros. Sci.* **7**, 563-578 (1967).
10. D. G. Lees and J. M. Calvert, "The use of  $^{18}\text{O}$  as a tracer to study the growth mechanisms of oxide scales", *Corros. Sci.* **16**, 767-774 (1976).
11. G. B. Gibbs and R. Hales, "The influence of metal lattice vacancies on the oxidation of high temperature materials", *Corros. Sci.* **17**, 487-507 (1977).
12. A. M. Pritchard, N. E. W. Hartley, J. F. Singleton and A. E. Truswell, "Oxygen-18 and deuterium profiling in thick films on Fe-9% Cr alloys by 3 MeV nuclear microprobe", *Corros. Sci.* **20**, 1-17 (1980).
13. A. Atkinson, "Transport processes during the growth of oxide films at elevated temperature", *Rev. Mod. Phys.* **57**, 437-470 (1985).
14. A. Atkinson, "Wagner theory and short circuit diffusion", *Mater. Sci. Technol.* **4**, 1046-1051 (1988).

